GPHS 446 | Project
Oceanographic Noise at Taranaki Coast

Irshad Ul Ala | Student ID 300397080
Victoria University of Wellington

October 3, 2021

1 Abstract

2 separate, month long datasets of various seismometer pairs were considered and compared for cross correlation. Additionally, 2 different general orientations of seismometer pairs (perpendicular and parallel to Taranaki coastline) were considered for each time frame. Perpendicular arrangements appeared to produce relatively clearer plots for 2020, but poorer plots in 2021, leading us to conclude that there was no particular advantage to either. Instead, the ideal conditions for a cross correlation plot to examine oceanographic noise near Taranaki coastline appear to be met using the HIZ/TSZ seismometer pair located NorthEast of Mt Taranaki ; a seismometer pair distance of approximately 60-70km would likely be the most significant factor in explaining that.

---

2 Introduction

Oceanographic noise is a very important key to understanding the nature of idle oceanic processes. This importance is even more evident when we consider the fact that electromagnetic waves do not travel as efficiently across the ocean. Low frequency sound waves, particularly are consistently picked up on seismometers (due to low attenuation across long distances), but rarely extensively studied. In this paper, we review some of the basic terminology and understanding behind Green's function, typical ambient and oceanographic noise, and how methods typically used in ambient noise tomography are being used to attempt to examine said oceanographic noise.

Ambient noise tomography leverages the idea that one can directly measure the impulse response using **Green's function**. Assuming the sources of the ambient noise are evenly distributed, the Green's function between two points of interest can be estimated from the cross-correlation of seismometer recordings (Weaver Lobkis 2001a,b, 2004). In our case, we will be using multiple pairs of seismometers' **ambient noise** recordings to **cross correlate** against. These cross correlations (correlalograms) could then be used to try understand the oceanographic noise.

This study will be looking at pairs of stations near the Taranaki coast to try understand the oceanographic noise there, and the ideal conditions for extracting good cross correlation plots with a distinctively high signal to noise ratio (SNR). We shall consider if there is any change in quality of oceanographic noise detected through basic cross correlation plots in the same time period between years 2020 and 2021, with 2 different alignments.

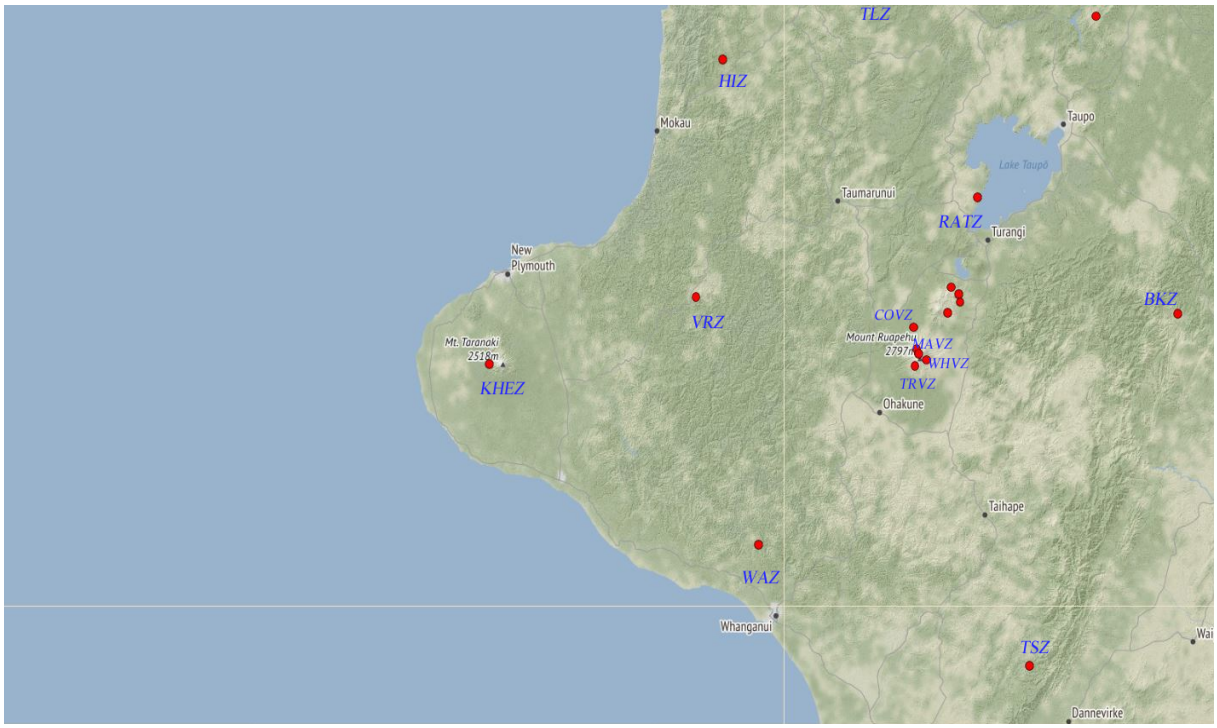

Figure 1: Visual Comparison between convolution, cross correlation and autocorrelation (GEONET map depicting most if not all of the stations used for cross correlation tests in this paper

In the spirit of experimentation, we are going to try 2 different alignments of station pairs, in 2 different time periods : 1/6/2020-1/7/2020 and 1/6/2021-1/7/2021. The first alignment will be seismometer pairings that are roughly parallel to the Taranaki coastline, while the 2nd alignment will be pairings roughly normal/perpendicular to it.

3 Theory

3.1 Cross Correlation

Cross correlation is conducted over long sets of data to typically enhance a common shorter period event withing that trace.

$$f \bigstar g \equiv \bar{f}(-t) * g(t) = \int_{-\infty}^{+\infty} \bar{f}(-\tau) g(t-\tau) d\tau = \int_{-\infty}^{+\infty} \bar{f}(\tau) g(t+\tau) d\tau \tag{1}$$

Cross correlation is equivalent to the of the convolution between the conjugate of the first function f (denoted by $\bar{f}$) and g, without flipping the function f (which is why it is denoted by $\bar{f}(-t)$.

Visually, cross correlation is represented by directly coalescing 2 curves together (without flipping either curve), to constructively superpose the bits that match, and destructively superpose the bits that do not match.

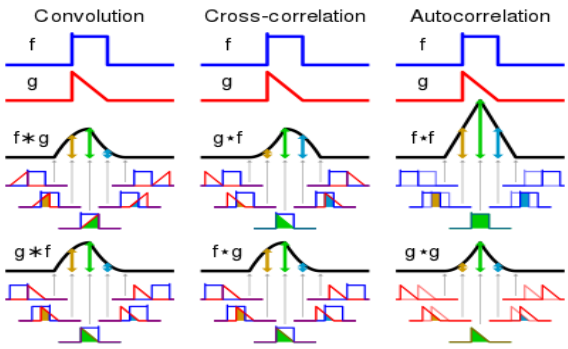

Figure 2: Visual Comparison between convolution, cross correlation and autocorrelation ("Cross-correlation - Wikipedia", 2021)

Considering that interpretation, one could argue that cross correlation is conceptually the easiest of the 3 common forms of function superposition.

3.2 Green's functions

Green's function is often touted as a mathematical trick to solve an 2nd order Ordinary Differential Equation of the form:

$$\frac{d^2u}{d^t} + k(t)\frac{du}{dt} + p(t)u(t) = f(t) \tag{2}$$

which is a standard inhomogeneous, linear ODE, with

the initial conditions $u(t=0) = u_0$ and $\frac{du}{dt}|_{t=0} = v_0$

One of the most common steps to solving such ODEs, is to first consider the simpler, homogeneous case. Suppose that we already knew the solution of the homogeneous solution to be $u_1(t)$ and $u_2(t)$. Then, the inhomogeneous solution would be of the form:

$$u(t) = C_1 u_1(t) + C_2 u_2(t) + u_p(t)$$

where $u_p(t)$ is any particular solution for the inhomoegeneous component of the equation. After determining this particular solution, one can use the initial conditions to find the coefficients for the general solution.

3.2.1 $\mathbf{u}_p(t)$

The process of finding the particular solution is difficult and is commonly done with one of 2 methods : inference, or variation of parameters. With inferences, every new guess involves seeing if the new guess of $u_p(t)$ creates a version of f(t), one has to create another, better version of $u_p(t)$. The other method, variation of parameters, is typically a laborious endeavour.

This process can get very difficult if one has a complicated f(t).

3.2.2 Simplifying f(t) using Dirac's equation

Green's function helps alleviate the difficulty from the complexity of f(t).

This begins by finding a general expression that indicates what $u_p(t)$ is for any $f(t)$ that we conceivably would use. Let us start by decomposing f(t) into 2 simpler functions, $f_1(t)$ and $f_2(t)$. Equivalently, $u_p(t)$ will be decomposable into $u_{p1}(t)$ and $u_{p2}(t)$. What Green's function involves is making essentially, an "infinite sum of particular solutions".

A very good way to do this is to use the Dirac's equation, which describes a point specific function that is zero at all other points except at one infinitesmall point such that:

$$\int_{-\infty}^{+\infty} \delta(x)dx = 1 \tag{3}$$

This function is commonly used to describe probability **mass** functions like Poisson, whereby a function is otherwise 0, except at specific points. Regardless of how large the instance of the event, a typicaly continuous distribution would not be able to yield a non-zero output at any given single point, since that goes against the definition of the point being "infinitesmall". The Dirac function allows one to conceptualise a distinct, significant event in an otherwise continuous function.

Using the Dirac's function allows one to simply split any given f(t) into:

$$f(t) = \int_0^{+\infty} d\tau\ \delta(t-\tau) f(\tau) \tag{4}$$

which describes f(t) being a sum of distinct, "spiked" events, where the size of the kick at a time $t = \tau$ is f(τ). So, if we are able to solve the 2nd order ODE for 1 given "spiked" event at time t=τ, one could conceivably solve the entirety of f(t) since each "spiked" event has the same form, just at a different time.

3.2.3 What Green's function is

The Green's function is the **solution** to the inhomogeneous equation

$$\frac{d^2G(t,\tau)}{dt^2} + k(t)\frac{dG(t,\tau)}{dt} + p(t)G(t,\tau) = \delta(t-\tau) \tag{5}$$

Additionally, the Green's function, G, also needs to satisfy the initial conditions $G(t=0,\tau) = 0$, $\frac{dG}{dt}|_{t=0} = 0$, the homogeneous version of the initial conditions for the parent 2nd order ODE. This homogeneity allows one to use a simple manipulation of the overall solution u(t) later on.

With said G(t, τ) solution,

$$u_p(t) = \int_0^{+\infty} d\tau G(t,\tau) f(\tau) \tag{6}$$

leading to the overall solution:

$$u(t) = C_1 u_1(t) + C_2 u_2(t) + \int_0^{+\infty} d\tau G(t,\tau) f(\tau) \tag{7}$$

where C_1 and C_2 have to chosen such that

$$u(t=0) = C_1 u_1(0) + C_2 u_2(0)$$

$$\frac{du}{dt} = C_1 \frac{u_1(t)}{t}|_{t=0} + C_2 \frac{u_2(t)}{t}|_{t=0}$$

The final integral term has 0 for both initial conditions, allowing us to manipulate just C_1 and C_2 to match the initial conditions that we wish to match, instead of **consistently solving for different Gs**.

This Green's function enables one to understand the origin of a physical process. A simple example would be u(t) describing the position of a ball with mass 1, and the ODE in question is Newton's 2nd law. Suppose there was a drag force ($=k(t)\frac{du}{dt}$), and an elastic force ($=p(t)u(t)$), then f(t) in this case would describe the external force applied to the ball at t. Hence, the green's function G(t,τ) would be the location of the ball, assuming it starts at the origin and at rest - because of the initial conditions we require

the Green's function to have. Likewise, by extracting the Green's function from the ambient seismic noise recorded at two stations one can understand something about the ambient seismic field and resolve the noise into useful research data.

3.3 Ambient Noise

Green's function retrieval commonly relies on cross-correlating the ambient noise that is simultaneously recorded at 2 or more stations. Several studies at this point have demonstrated that cross-correlating the coda of ambient noise cross-correlation functions enables reconstruction of the Green's function, regardless of the operating time of the stations (Lin et al., 2007). Typically, studies involve filtering said obtained Green's functions to compute Rayleigh wave group dispersion curves at periods of one's choosing. Due to the limited scope of this project, we will not be going beyond a simple examination of the cross correlation plots.

One of the main reasons for interest in extracting the Earth's Green's function for ambient noise is the fact that it removes the need for explicitly extracting the source's characteristics. The cross-correlation concerning 2 seismometers of noise signatures originating from a source (such as the ocean), one may retrieve the impulse response function between these two seismometers. Ideally, only source contributions from stationary arrivals will interfere constructively in the spatial averaging, with all other unrelated arrivals being canceled.

Ambient noise is also a convenient, cheap, and readily available resource that can examined essentially anywhere with a readily stationed seismometer. While most studies to date have been conducted in continental settings, oceanic applications of ambient noise correlation should be equally as feasible and reasonable to do. In fact, most stations across Pacific islands typically detect Rayleigh wave Green functions originating from the ocean.

In our case, we are similarly going to examine how ocean waves, might be forming surface waves that are picked up as ambient noise in nearshore seismometers, by Mount Taranaki. Another important aspect of the study that needs to be maintained is the directionality of the seismometer pairs chosen. If the pairs chosen are of different orientations, the noise profiles may be difficult to compare. Hence, we consider 2 alignments of seismometers to conduct this cross correlation experiment in: perpendicular, and parallel to the coastline of interest.

4 Materials and Methods

All data was extracted from the GEONET station directory, using obspy. Data of concern was dated between 1st June and 1st July of 2020/2021, with broadband seismometers: KHEZ, WAZ, VRZ, HIZ, TLZ, RATZ, TMVZ, COVZ, MAVZ, TRVZ, BKZ, TSZ, MRZ, and WHVZ.

We are going to be conducting 2 alignments of sets of broadband seismometers, normal to each other. The first alignment of paired seismometers are parallel to the coastline, while the second alignment are perpendicular to it.

In addition to that, the time periods for these cross correlations are going to be 1st June 2020 - 1st July 2020, and 1st June 2021 - 1st July 2021.

5 Results

We begin by considering cross correlation curves of seismometer couples that are parallel to Mt Taranaki. All readings were taken with a sampling rate of 20Hz. Additionally, a pre-filter of (0.25,1) was applied for all cross correlations. Adjustments were however made, for some of the prefilters to better discern a Green's function from the plots, especially in the cross correlation plots for perpendicular arrangements in 2020 dataset.

5.1 Cross Correlations for parallel to Taranaki coastline | 2020

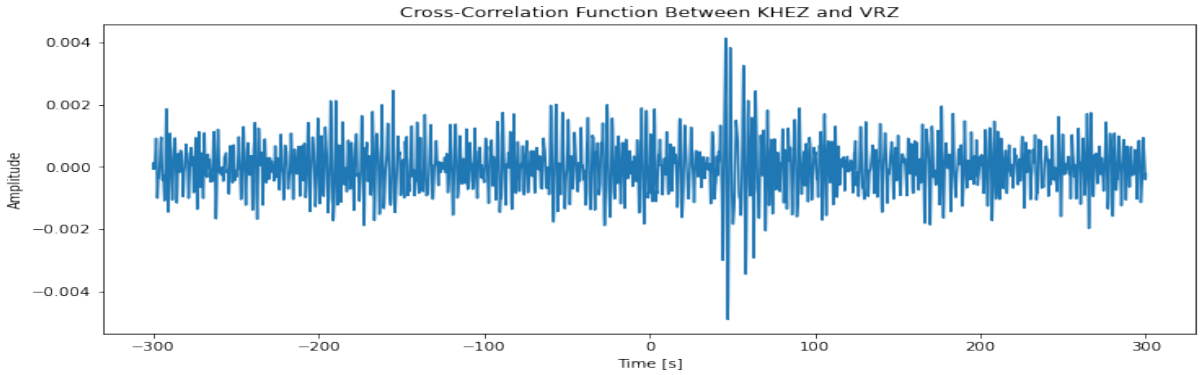

Figure 3: Cross correlation between KHEZ and VRZ. Stations are located approximately 66.83km from one another.

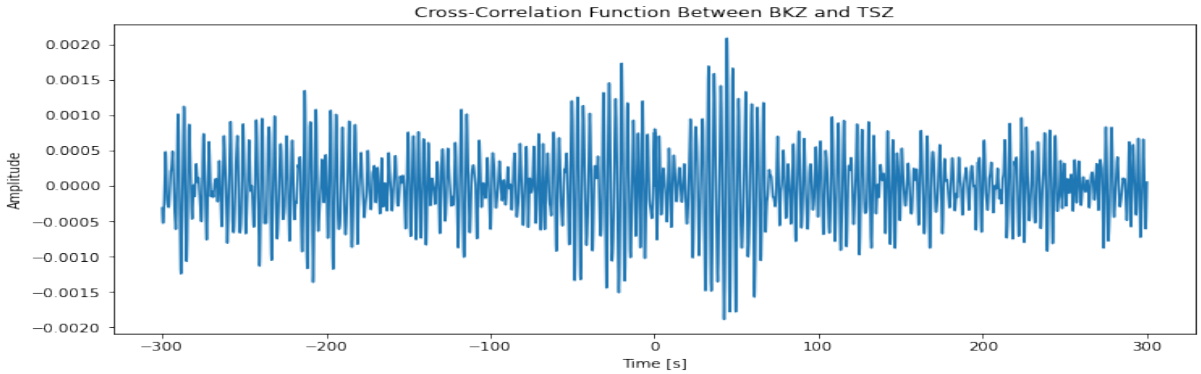

Figure 4: Cross correlation between BKZ and TSZ. Stations are located approximately 109.22km from one another.

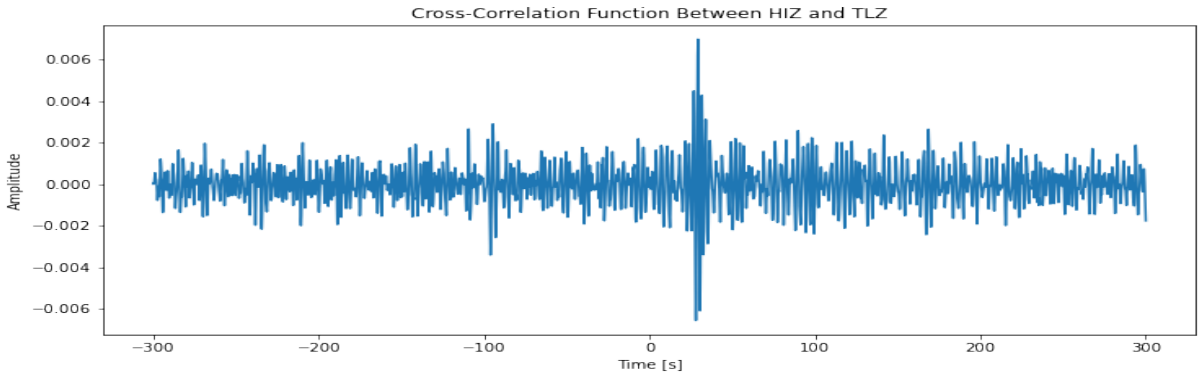

Figure 5: Cross correlation between HIZ and TLZ. Stations are located approximately 62.84km from one another.

5.2 Cross Correlations for perpendicular to Taranaki coastline | 2020

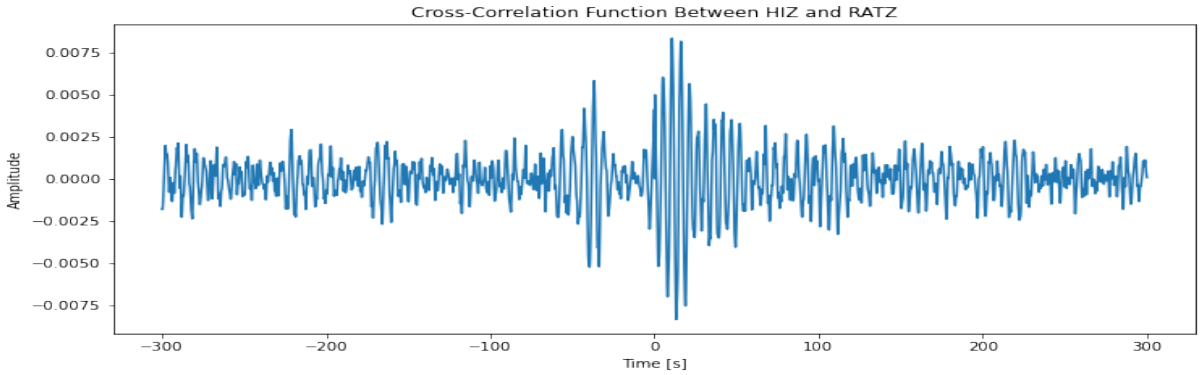

Figure 6: Cross correlation between HIZ and RATZ. Stations are located approximately 88.73km from one another.

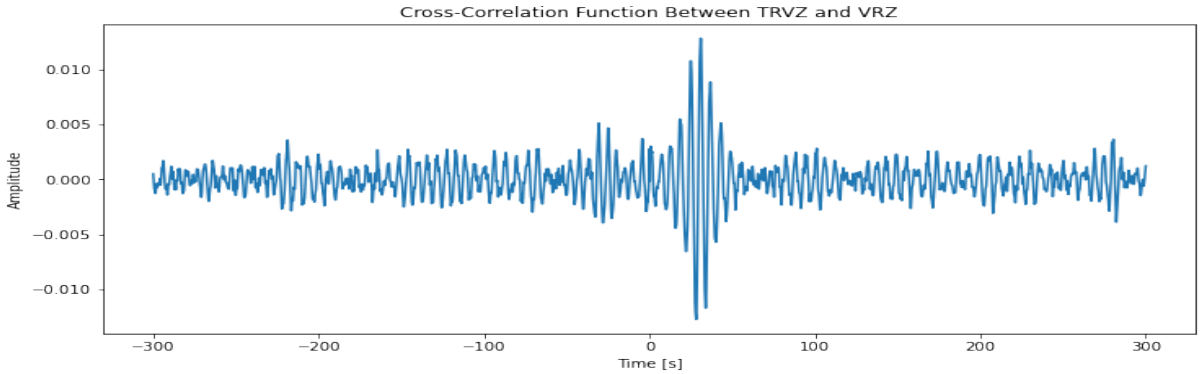

Figure 7: Cross correlation between TRVZ and VRZ. Stations are located approximately 70.72km from one another.

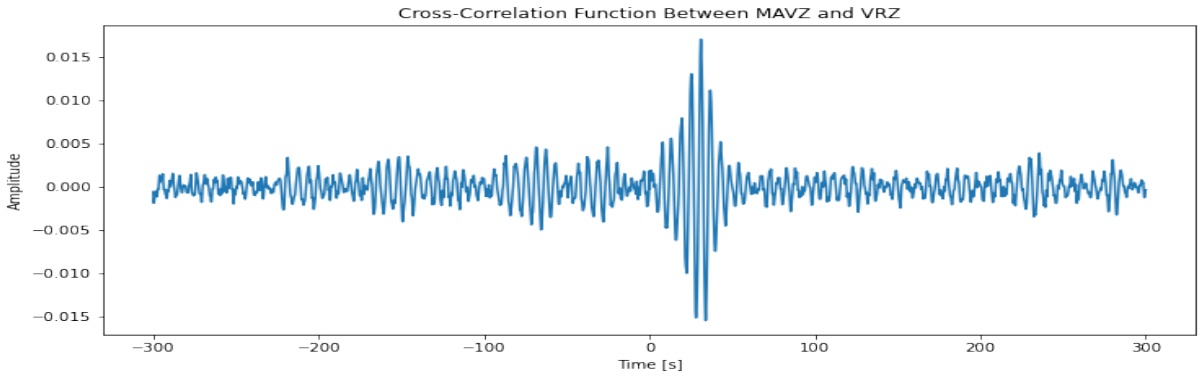

Figure 8: Cross correlation between VRZ and MAVZ. Stations are located approximately 71.03km from one another.

5.3 Cross Correlations for parallel to Taranaki coastline | 2021

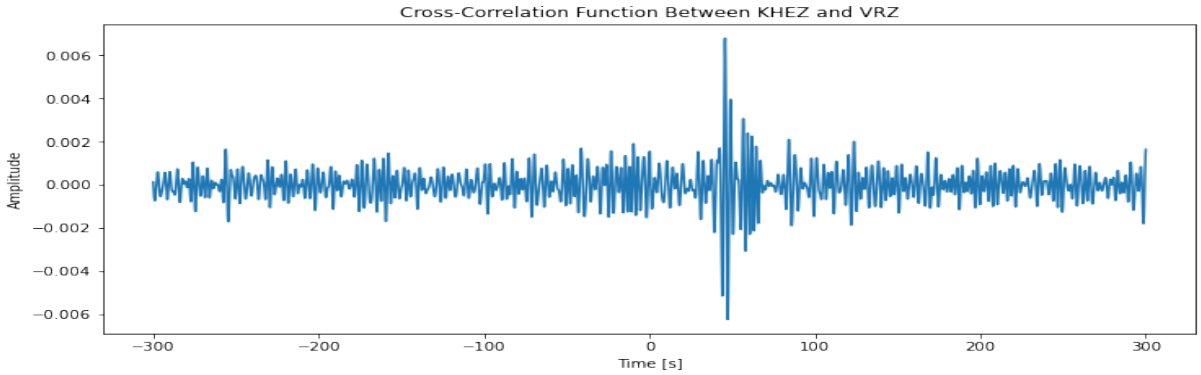

Figure 9: Cross correlation between KHEZ and VRZ. Stations are located approximately 66.83km from one another.

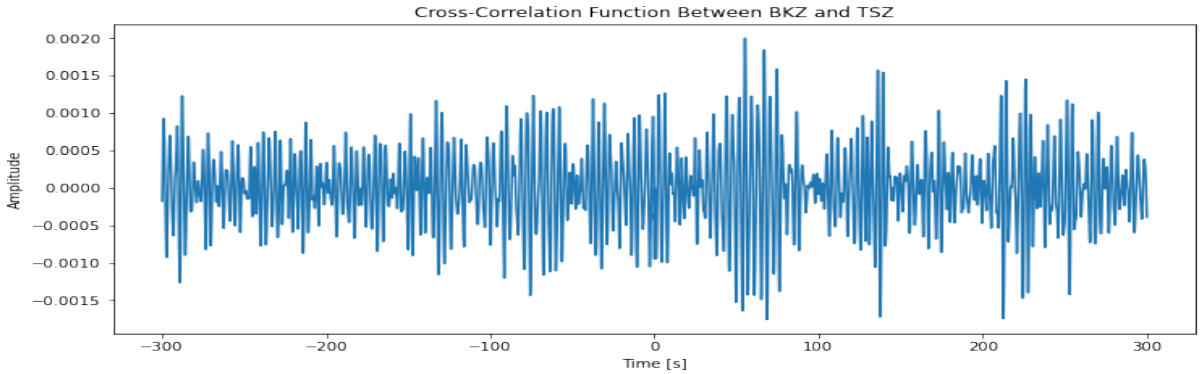

Figure 10: Cross correlation between BKZ and TSZ. Stations are located approximately 109.22km from one another.

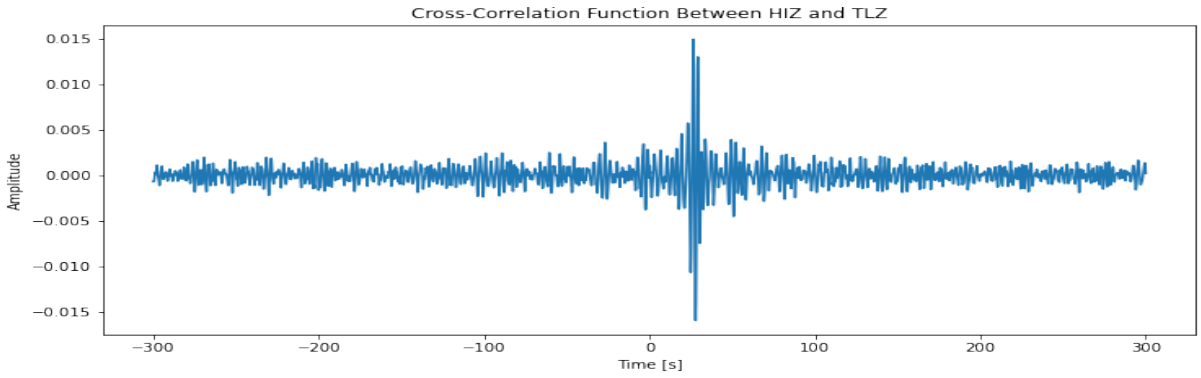

Figure 11: Cross correlation between HIZ and TLZ. Stations are located approximately 62.84km from one another.

5.4 Cross Correlations for perpendicular to Taranaki coastline | 2021

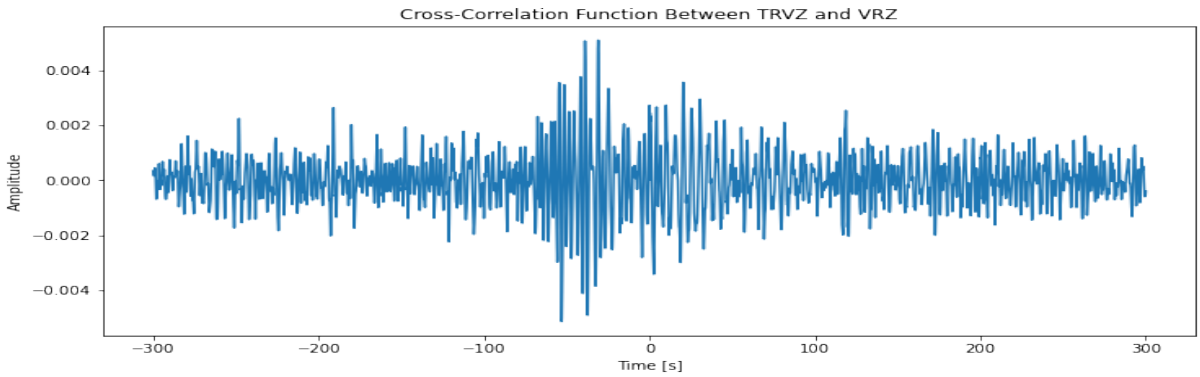

Figure 12: Cross correlation between TRVZ and VRZ. Stations are located approximately 70.72km from one another.

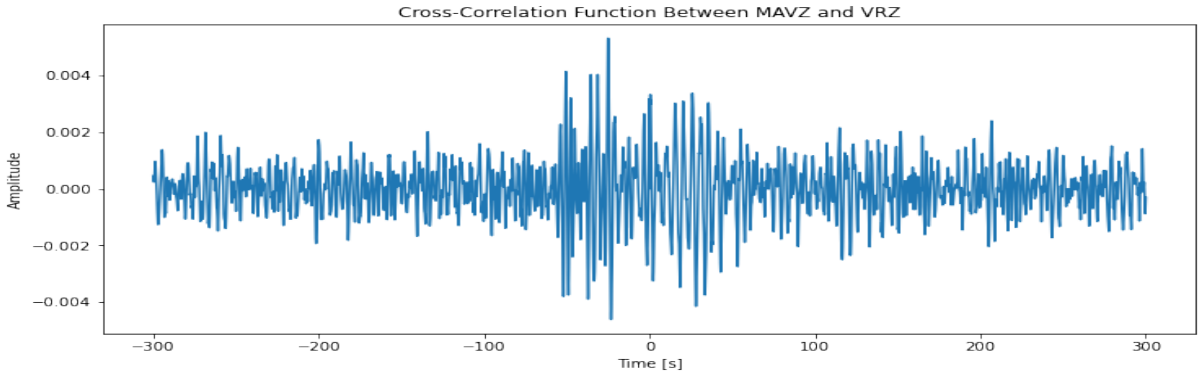

Figure 13: Cross correlation between MAVZ and VRZ. Stations are located approximately 71.03km from one another.

6 Discussion

6.1 Varying quality of data

Generally, the perpendicular pairs of seismometers appear to reproduce cross correlations with a better signal to noise(SNR) ratio, especially from the 2020 dataset. However, for the 2021 dataset, the parallel configurations appear to be reproduce clearer cross correlations. However, there must be some additional process or other source that causes the same seismometer pairs produce worse cross correlations in 2021 versus 2020 for the perpendicular alignments(TRVZ and VRZ, MAVZ and VRZ), while producing arguably cross correlation plots with better SNR for the parallel alignments (HIZ and TLZ, KHEZ and VRZ).

The HIZ/TLZ pair appear to have cross correlation signals with the best SNR likely due that pair strictly being more North-Westernly compared to the other pairs. Pairs such as HIZ/RATZ for instance, appear to produce poorer correlation plots possibly due to additional source(s) of noise such as Lake Taupo. More Southerly pairs of seismometers in general, appear to suffer from poorer SNR correlation plots as well.

While typically ill advised, some correlation plots were made for seismograms that are much closer together, with an example shown in Figure 16 between COVZ and TRVZ. Another example was shown of a pair of seismometers being apparently too far to effectively capture a systematic noise source, specifically from the Taranaki coast alone in Figure 14 between KHEZ and TSZ.

Among the seismometer pairs, it is worth noting that the BKZ and TSZ pair appears to perform the worst for this cross correlation experiment likely because it is located the furthest from the Taranaki coast, and is picking up too many other noise sources to resolve appropriately. However, another possibility is that the pairwise distance between the 2 seismometers in this case is too high, leading to a poor reconstruction of the Green's function. In fact, looking at the distances between all the pairs of seismometers, it would appear that the ideal separation distance for 2 seismometers to create a distinct cross correlation plot would be around 60-70km.

Most of the other pairs appear to reproduce Green's functions quite well. It would perhaps be wiser to consider other orientations of datasets, this paper only considers HHZ data, but LTZ, HHN and HHE could perhaps be considered. Additionally, due to the time constraint, only

month long datasets were used. Perhaps, longer datasets could have been considered.

6.2 Sources of noise

From the cross correlation plots above, there appears to be a systematic set of oceanic noise from the coast of Taranaki. Further study on the surface waves generated at the coast of Taranaki would likely return a fruitful, more in depth discussion about the nature of surface waves generated by the Mt. Taranaki coastline.

Generally, oceanographic noise could arise due a variety of reasons including: sounds produced and used by living marine resources, natural sources of noise from physical oceanographic processes and anthropogenic noise sources. Given the time period of data in consideration however, it is likely that the noise sources of interest are simple long period physical oceanographic sources.

Without further examination of the data, however, it would not be possible to make any further inferences about the sources of noise in our dataset.

7 Conclusion

Generally there appears to be discernable noise source along Taranaki coast, and possibly Lake Taupo. It is not entirely clear yet why there appears to be discrepancies in the quality of the data obtained between 2020 and 2021, however, perhaps a longer time series for the data would have produced better, more consistent results.

Additionally, it is evident that taking data from pairs of seismometers that are below say 40km apart, is too unwieldy for any oceanographic noise examination, and the same could be said for seismometers over about 120km apart.

The specific orientation of the pairwise seismometers does not appear to have much bearing on the quality of the prospective cross correlation plots, compared to the length of data taken, sampling frequency, distance between the seismometers, and the location of the pair of seismometers. One could conceivably get much clearer cross correlation plots from making the pair of seismometers in question as Northwesterly as possible (as HIZ/TLZ pair is in Figures 5 and 11). Taking to this advice too far could possibly lead one to stray far from examining the Taranaki coast however.

Unfortunately, due to the limited scope of this paper, there is not much more information one could draw from the given analysis above about the surface waves created by oceanographic noise in Taranaki coast. However, the parameters required for consideration to ensure the best quality cross correlation plots, amongst the obvious frequency parameters appear to be location dependent and seismometer pair distance dependent for the most part. This information could possibly be useful to consider for future analysis.

8 References

Cross-correlation - Wikipedia. En.wikipedia.org. (2021). Retrieved 29 September 2021, from https://en.wikipedia.org/wiki/Cross-correlation.

Lin, F., Ritzwoller, M., Townend, J., Bannister, S., Savage, M. (2007). Geophysics Journal International [Ebook]. Retrieved 3 October 2021, from http://epsc.wustl.edu/~ggeuler/reading/cam_noise_biblio/lin_ritzwoller_townend_bannister_and_savage_2007-gji-ambient_noise_rayleigh_wave_tomography_of_new_zealand.pdf.

Weaver, R.L. Lobkis, O.I., 2001a. Ultrasonics without a source: Thermal fluctuation correlation at MHZ frequencies, Phys. Rev. Lett., 87, 134 301.

Weaver, R.L. Lobkis, O.I., 2001b. On the emergence of the Green's function in the correlations of a diffuse field, J. Acoust. Soc. Am., 110, 3011– 3017.

Weaver, R.L. Lobkis, O.I., 2004. Diffuse fields in open systems and the emergence of the Green's function, J. Acoust. Soc. Am., 116, 2731– 2734.

9 Acknowledgement

Code used to produce the cross correlation plots is available separately and is mostly taken from ROSES unit3 | Seismic Tomography.

10 Appendix

10.1 Additional cross correlation plots for staions that were too far apart

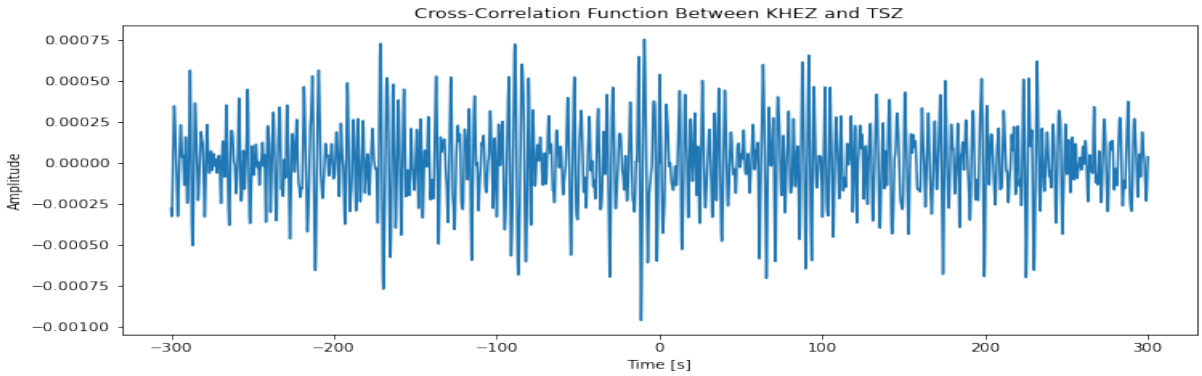

Figure 14: Cross correlation between KHEZ and TSZ for perpendicular alignment in 2021/6 - 2021/7. Stations are located approximately 187.02km from one another.

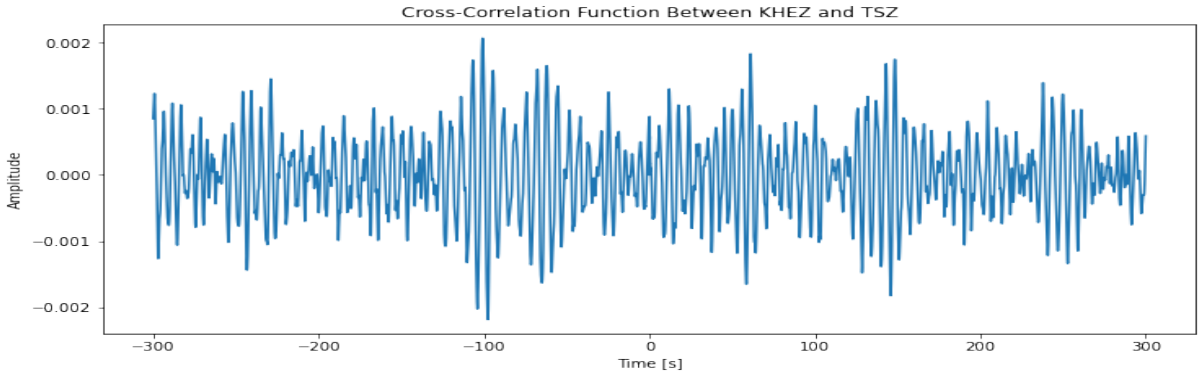

Figure 15: Cross correlation between KHEZ and TSZ for perpendicular alignment in 2020/6 - 2020/7. Stations are located approximately 187.02km from one another.

10.2 Additional cross correlation plots for staions that were too close

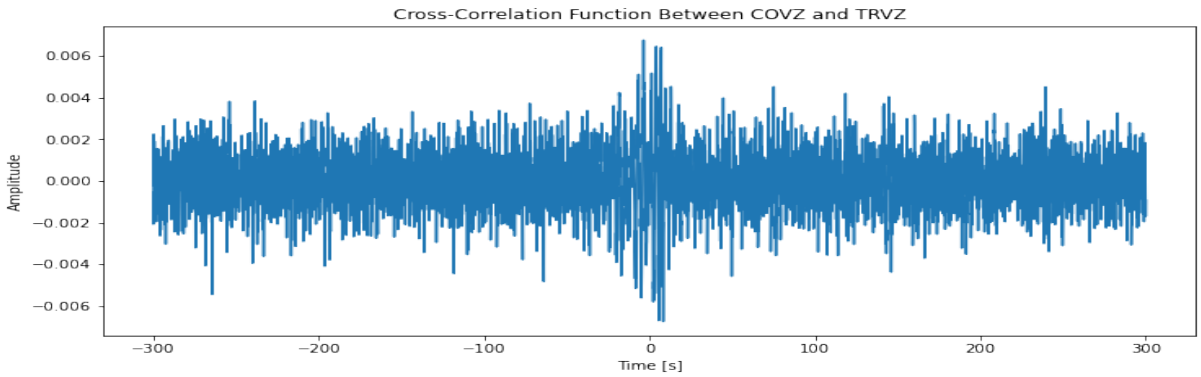

Figure 16: Cross correlation between COVZ and TRVZ. Stations are located approximately 11.01km from one another.

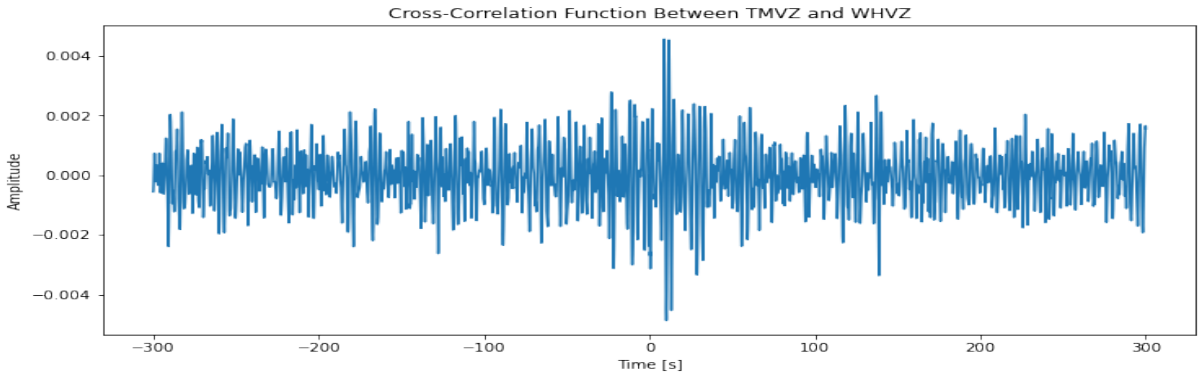

Figure 17: Cross correlation between TMVZ and WHVZ. Stations are located approximately 21.06km from one another. 2020/6-2020/7.

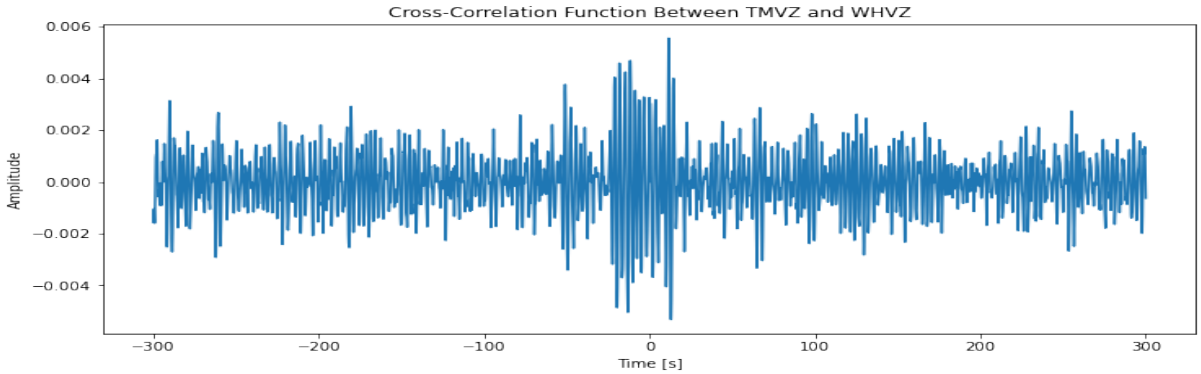

Figure 18: Cross correlation between TMVZ and WHVZ. Stations are located approximately 21.06km from one another. 2021/6-2021/7.